

Parameters affecting the homogeneous and heterogeneous degradation of quinoline solutions in light-activated processes

Alexei Nedoloujko¹, John Kiwi^{*}

Institute of Physical Chemistry II, Swiss Federal Institute of Technology, Lausanne 1015, Switzerland

Accepted 20 May 1997

Abstract

The light-activated degradation kinetics of quinoline were studied in detail on Hg lamp and Suntest solar-simulated irradiation. Fenton-photoassisted mineralization in homogeneous solution with a peroxide to quinoline ratio of approximately 50 (quinoline, approximately 1 mM) was complete in about 30 min on Hg lamp irradiation. Reactions activated by a solar simulator led to 80% mineralization of the same quinoline solutions within the same time period due to a lack of a strong UV component. Heterogeneous photocatalytic TiO₂-mediated degradation proceeded at a slower rate than the homogeneous reaction. The influence of a number of factors, such as the substrate concentration, solution pH, gas atmosphere and dynamics of H₂O₂ addition, was investigated. The stoichiometry of the mineralization reaction was analysed as a function of the gas atmosphere used. Quinoline degradation was possible via dark and light-activated reactions. Quinoline did not affect the H₂O₂ consumption rate in the presence of Fe³⁺ ions. This suggests that, during degradation, the reaction of Fe³⁺ ions with H₂O₂ is the rate-determining step. Quinoline did not complex with Fe³⁺ ions in the dark. However, complex formation occurred during photodegradation with Fenton-like reagents, such as Cr⁶⁺ or Cu²⁺ ions and combinations of Cu²⁺ + Fe³⁺ ions, in the presence of H₂O₂. The latter systems were compared with the classical Fenton reagent leading to quinoline mineralization. © 1997 Elsevier Science S.A.

Keywords: Ferric ions; H₂O₂ decomposition; Photoassisted mineralization; Quinoline; Steady state kinetics

1. Introduction

Homogeneous and heterogeneous photocatalyses have been developed in recent years for the efficient detoxification of wastewater [1–4]. These approaches provide an alternative to filtration, reverse osmosis and incineration in environmental cleaning processes. In this work, OH[•] radicals were generated via homogeneous and heterogeneous systems, and the interaction of photons with quinoline, leading to the mineralization of this compound, was examined. Several studies have shown that Fenton-like reactions are efficient in the degradation of organic compounds and that these processes are enhanced by light irradiation [5].

Quinoline is present in the effluents of the oil, chemical and pharmaceutical industries, and presents carcinogenic, toxic and recalcitrant properties. The techniques of ozonization [6], dark H₂O₂ oxidation [7], groundwater removal [8], bacterial degradation [9] and mixed bacterial strands [10] have been applied over the last 10 years for the degradation

of quinoline in the dark. In this study, we investigate the accelerated degradation of this substance via advanced oxidation technologies (AOTs).

2. Experimental section

2.1. Materials

Quinoline (Fluka) was used as received. FeCl₃ and H₂O₂ were of Fluka p.a. grade and were used as received, together with Na₂CrO₄ and Cu(NO₃)₂. P-25 Degussa TiO₂ with a surface area of 55 ± 5 m² g⁻¹ was used.

2.2. Photoreactor and irradiation devices

The irradiation of the solutions was carried out in cylindrical flasks (volume, 60 ml) using 40 ml of solution in each case. The gases evolved during the reaction were measured in the 20 ml dead space above the solution. Two sources of light were used:

1. a Suntest solar simulator provided with an Xe lamp (1500 W) with a spectral distribution resembling the solar spec-

^{*} Corresponding author.

¹ On leave of absence from the A.N. Bach Institute of Biochemistry, Leninsky Pr. 33, Moscow 117071, Russia.

trum (300–800 nm) and a white light equivalent output of 96 mW cm^{-2} ;

- an Hg medium pressure lamp (400 W) with an output between 250 and 450 nm and a white light equivalent output of 250 mW cm^{-2} ; about 50% of the radiant UV energy is emitted at 366 nm (15 W equivalent electric power).

The temperature during the experiment was approximately 46–47 °C. The irradiated surface corresponds to the total solution surface (36 cm^2).

2.3. Analyses

Peroxide left in the solution was determined by the Merckoquant® peroxide test and by permanganate titration [11]. The absorption spectrum of the permanganate solution used is shown in the inset of Fig. 1; permanganate absorbs between 400 and 600 nm. This method is adequate for the H_2O_2 determination in solutions containing iron salts (Fenton reagent) which absorb light at $\lambda < 450 \text{ nm}$, i.e. not allowing the application of the iodide method. No effect of FeCl_3 on MnO_4^- reduction was observed. The permanganate in solution had a molar absorption coefficient (ϵ) of $2240 \text{ M}^{-1} \text{ cm}^{-1}$ at 526 nm. The value of H_2O_2 remaining in solution was found via the relation $2\text{KMnO}_4/5\text{H}_2\text{O}_2$. Fig. 1 shows the linear dependence between the optical density (D_{526}) and the amount of peroxide consumed. Permanganate (0.8 mM) at $\lambda = 526 \text{ nm}$ showed an optical density D of 1.80 in a 1 cm cell. This solution was acidified with sulphuric acid (11%) to avoid precipitation of MnO_2 . The H_2O_2 was determined in the range 0.1–13 mM after a 5 min reaction period.

Nitrate and nitrites were determined in a Tecator titrator using sulphanilamide and detecting the colour intensity of

the solution spectrophotometrically at 540 nm. The ammonium ion present was assessed via the Merckoquant® ammonium test. The lower limit of detection was 10 mg l^{-1} . Total organic carbon (TOC) was monitored via a Shimadzu 500 instrument. Spectrophotometric analysis was carried out using a Hewlett-Packard 8452A diode array. The detection of CO_2 was performed using a Gow-Mac thermal conductivity detector with He as carrier gas and a Poropak Q column.

3. Results and discussion

3.1. Non-complexation between quinoline and Fe^{3+} ions in solution. Protonation of quinoline at acidic pH

Fig. 2 shows the spectra of quinoline solutions in the presence of various concentrations of FeCl_3 . The increase in optical density in Fig. 2 is due to the absorption of the added Fe^{3+} ions. It can be seen that, when FeCl_3 is added to quinoline, no changes in the absorption spectrum are observed and no complex formation occurs. Furthermore, no decrease is observed when quinoline– FeCl_3 solutions are aged for several days in the dark, indicating that no long-term complexation occurs. The spectra of the quinoline solutions were also recorded on addition of $\text{Fe}_2(\text{SO}_4)_3$ or $\text{Fe}(\text{ClO}_4)_3$ instead of FeCl_3 , but showed no observable complexation in either case.

The absorption spectra of quinoline in aqueous solution at various pH values are shown in Fig. 3. The protonated form absorbs more strongly in the near-UV since the N lone pair electrons form σ bonds with H^+ and cannot complex with the Fe^{3+} ions present

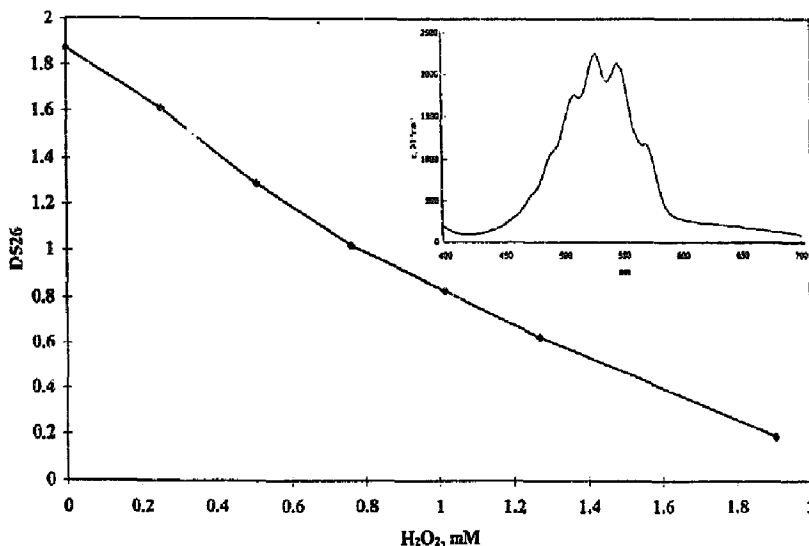


Fig. 1. Optical density of a permanganate solution (0.8 mM) (1 cm cell) at 526 nm vs. the amount of H_2O_2 consumed. The inset shows the absorption spectrum of the permanganate solution used.

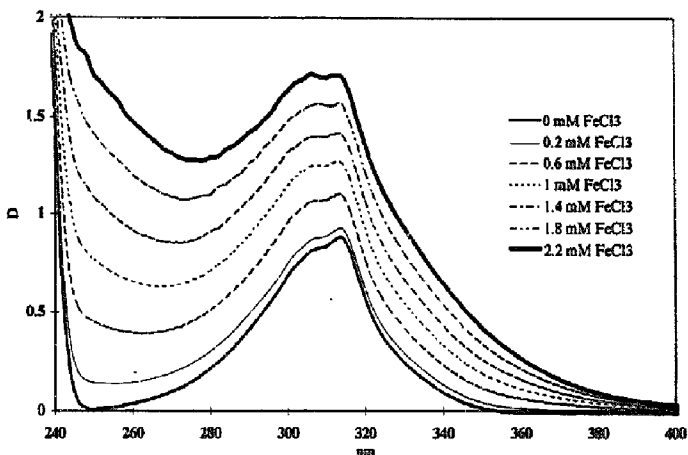


Fig. 2. Optical absorption spectra of solutions of aqueous quinoline (0.22 mM) at pH 2.7 as a function of the amount of FeCl_3 added.

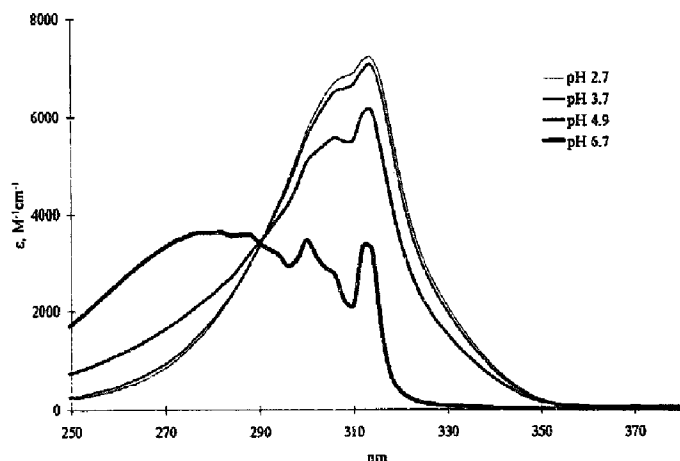
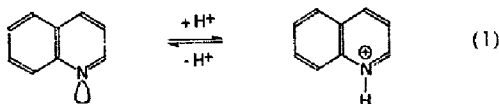


Fig. 3. Absorption spectra of quinoline solutions as a function of pH (for other details see text).



Therefore in aqueous solution (Fig. 3), quinoline exists in the protonated form at acidic pH values and, on moving to less acidic pH values, deprotonation occurs. Between pH 3 and pH 5, a colloidal solution is formed, which absorbs in the visible region as a function of the concentration of reactants used. Beyond pH 5, $\text{Fe}(\text{OH})_3$ formation occurs.

Processes mediated by Fenton reagent in acidic media have been shown to lead to the efficient degradation of organic pollutants [12–14]. Therefore it is of interest to examine the absorption properties of a quinoline solution as a function of the solution acidity. Quinoline is slightly soluble in water, but at acidic pH the solubility improves. At pH 2.7, the sol-

ubility at 20 °C is 37.5 mM or 5 g l^{-1} . The titration curve for quinoline is shown in Fig. 4. The protonation of quinoline shifts the absorption spectrum to longer wavelengths. The $\text{p}K_a$ value obtained from the second derivative in Fig. 4 is 4.7 ± 0.1 , in line with the dependence of the optical densities at 347 nm. This value is in reasonable agreement with the literature value of 4.90 [15]. The dependence of the optical density is taken at $\lambda = 347 \text{ nm}$ which is the wavelength of the laser used. Extensive work involving excitation at this wavelength has been reported previously [16].

3.2. Accelerated mineralization of quinoline via photoassisted Fenton reagent

The accelerated mineralization of quinoline via photo-Fenton processes is shown in Fig. 5. The aim of the experiment reported in Fig. 5 was to optimize the time necessary for quinoline degradation. This, in turn, minimizes the use of

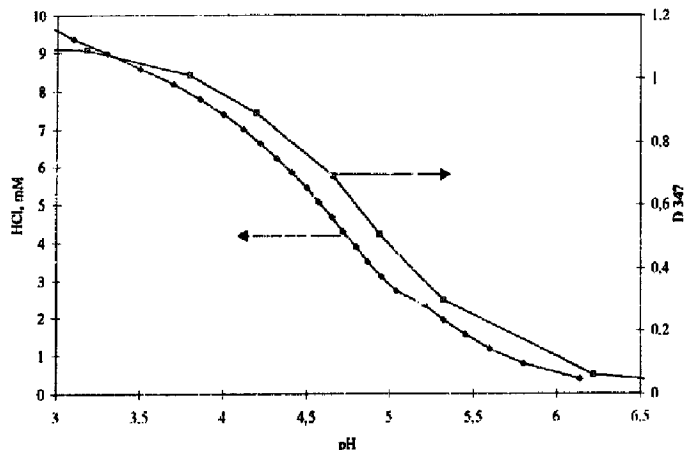


Fig. 4. Optical density at 347 nm of an 8.45 mM quinoline solution ($d=0.5$ cm) as a function of pH.

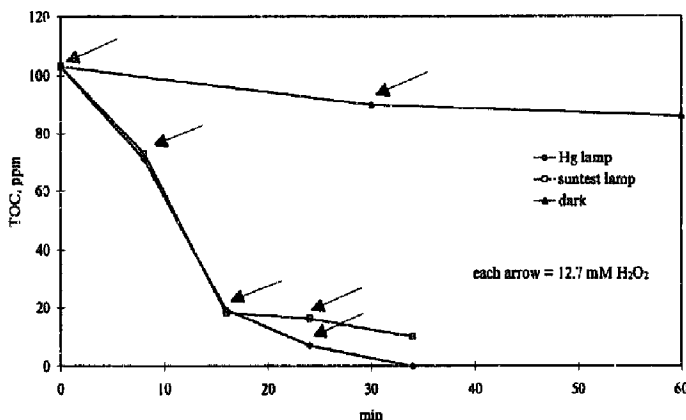


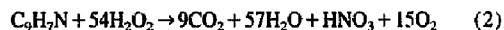
Fig. 5. Typical degradation profile as a function of time for a quinoline solution (0.95 mM) when H_2O_2 (12.7 mM) is added (see arrows) in the presence of $FeCl_3$ (1.5 mM) at pH 3. Hg lamp and solar simulator results are shown.

expensive UV–visible photons. This is important since photodegradation processes taking place within minutes have been reported to have the potential for economic utilization [2,3,10,13]. In the dark, the initial TOC is reduced by less than 10% (Fig. 5). When a 400 W Hg lamp (integrated light output, 250 mW cm^{-2}) and a 1500 W Xe lamp Suntest simulator (integrated light output, 96 mW cm^{-2}) are used, the mineralization kinetics are about the same up to 85% TOC decrease as shown in Fig. 5.

The possibility of the direct photodecomposition of H_2O_2 was checked during the course of these experiments. In the absence of Fe^{3+} , the rate of H_2O_2 consumption was more than an order of magnitude lower than in the presence of Fe^{3+} (as in Fig. 5).

The last slow photodegradation step observed beyond 17 min shows the difficulty in converting the N atom associated with quinoline into oxidized nitrogen compounds (see Section 3.6). Full mineralization is observed within approxi-

mately 30 min using the Hg lamp with a strong line at $\lambda = 366$ nm. The action spectrum of the photolysed solution changes during the course of the reaction due to the intermediates generated in the solution. The generated intermediates therefore seem to be affected by the strong UV Hg lines but not by the weaker UV component of the Suntest simulator. Slow photocatalytic degradation of compounds containing C–N bonds has been reported recently for formamide [17] and Orange II [18]. As shown in Fig. 5, the most suitable photodegradation time found is slightly above 30 min for a solution of quinoline (0.95 mM) requiring about 50.8 mM of H_2O_2 . The total degradation proceeds with an H_2O_2 to quinoline ratio of approximately 50 (Fig. 5). The approximate mineralization stoichiometry can be suggested as



The evolution of CO_2 and NO_3^- is reported in Section 3.6 (Fig. 10 and Fig. 11). The photodegradation process is

Table 1
Comparison of Fenton-like systems for the photodegradation of quinoline (on illumination with a 400 W mercury lamp)

System	Initial TOC (ppm)	TOC after two injections of H ₂ O ₂ (ppm)	Time necessary for the consumption of one portion of H ₂ O ₂ (12.7 mM) (min)
0.3 mM Na ₂ CrO ₄ , pH 4.8	120	88	> 120
1.5 mM Cu(NO ₃) ₂ , pH 3	110	87	99
0.75 mM FeCl ₃ + 0.75 mM Cu(NO ₃) ₂ , pH 3	110	26	30
1.5 mM FeCl ₃ , pH 3	103	19	8

strongly affected by the initial quinoline concentration. When a solution containing quinoline (1.20 mM) is irradiated with the Hg lamp, about 9% of the initial TOC is still present after 42 min and five H₂O₂ additions.

Other cations, such as Cr⁶⁺, Cu²⁺ and Cu²⁺ + Fe³⁺ were used, together with Fe³⁺ ions, in Fenton-like photoassisted reactions. The results are shown in Table 1. The most favourable TOC reduction is observed for the combination of Fe³⁺ + Cu²⁺. However, the initial amount of H₂O₂ in the solution is consumed over a longer time compared with Fe³⁺ ions alone. The couple Fe^{3+/2+} (0.77 V) therefore seems to provide the most suitable couple from the viewpoint of kinetic acceleration (see Eqs. (3)–(6) below). The experiments were carried out at pH ~ 3, since it was the most suitable pH for the cations reported in Table 1. When using Cu²⁺, the formation of Cu⁺ in solution was observed. However, it seems unlikely that it would be possible to obtain high rates of quinoline photodegradation with copper ions, since the reaction rate between H₂O₂ and re-oxidized Cu²⁺ has been reported to be slow [19,20].

3.3. Efficiency of hydrogen peroxide utilization. Effect of oxygen

In Fig. 6, H₂O₂ (30%) was present at a concentration of 12.7 mM. The consumption of H₂O₂ was followed via the

permanganate test and Merckoquant® peroxide paper. Both methods show similar results for the residual H₂O₂ (within the experimental error of the measurements). Fig. 6 shows the H₂O₂ concentration for an irradiated solution containing FeCl₃ and quinoline (1 mM) (a), no quinoline (b) and after preliminary quinoline oxidation (c). On light irradiation, the consumption of the H₂O₂ added initially takes between 8 and 10 min. Inefficient H₂O₂ consumption is observed during the dark reaction as shown in the inset in Fig. 6. The consumption of the oxidant and concomitant quinoline degradation are an order of magnitude slower compared with the light-induced reactions. The time necessary for H₂O₂ consumption during dark or light-activated reactions is not affected significantly by the addition of quinoline. The absence of a noticeable quinoline effect on H₂O₂ consumption suggests that H₂O₂ decomposition is due to the reaction

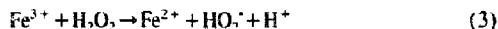


Fig. 6 suggests that quinoline does not enter into a complex with Fe³⁺ ions at the start of the reaction. This has been mentioned previously in Section 3.1. The formation of intermediates is observed due to the change in colour of the solution [20].

Kinetic plots of the decrease in TOC in the solution as a function of time for Ar-, air- and O₂-saturated solutions of

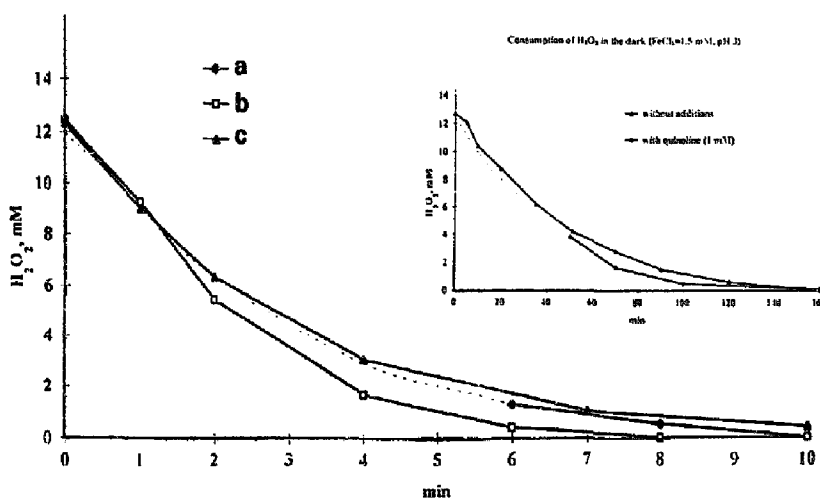


Fig. 6. Consumption of peroxide on exposure to light as a function of time for solutions of quinoline (1 mM) in the presence of FeCl₃ (1.5 mM) at pH 3. The inset shows the results of dark runs.

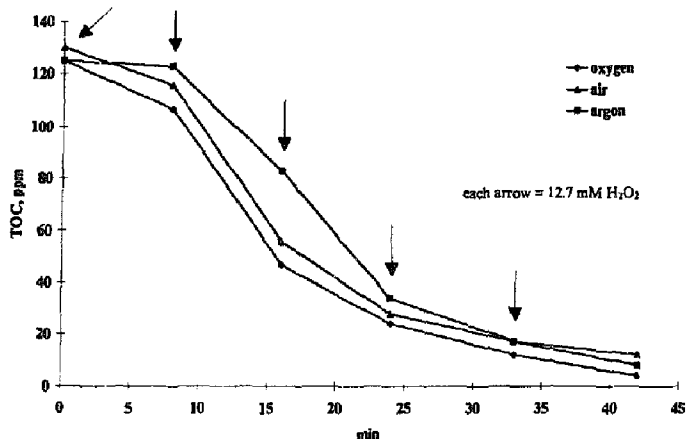
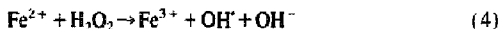


Fig. 7. Effect of gas atmosphere on the TOC values during the photodegradation of quinoline solutions (1.16 mM) in the presence of H_2O_2 (12.7 mM) and FeCl_3 (1.5 mM) (for other details see text).

quinoline are shown in Fig. 7. The gas atmosphere used has only a small effect on the photodegradation of quinoline. Therefore O_2 is not a very active oxidant compared with H_2O_2 in photoassisted Fenton reactions. The H_2O_2 consumption during quinoline degradation can be accounted for by reactions (3) and (4)

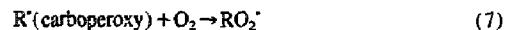


One electron is scavenged in the reduction of either HO_2 or OH^- radicals

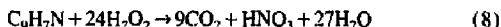


It can be suggested from reactions (3)–(6) that, if O_2 is a slow oxidative agent, it will only be marginally involved in the overall degradation process. If one electron is scavenged by one molecule of H_2O_2 , four molecules of H_2O_2 will be required per molecule of O_2 . In Section 3.2, Eq. (2) shows that the mineralization of one molecule of quinoline produces nine molecules of CO_2 and one molecule of nitrate. The concentration of Fe^{3+} ions used is approximately 50% higher than that of quinoline. Taking this and Eqs. (3)–(6) into account, the contribution of Fe^{3+} cations to the overall stoichiometry is negligible. In this case, the H_2O_2 to quinoline ratio will have a lower limit of approximately 48 if oxygen is not consumed during the degradation.

The information presented in Fig. 5 suggests that the ratio of H_2O_2 to quinoline changes during the course of the reaction. After two additions of H_2O_2 , this ratio is about 33 as indicated by the arrows in Fig. 5. This confirms the participation of oxygen during quinoline photodegradation. The most probable type of reaction will lead to the formation of carboxy or carboperoxy radicals [12,14,20]



In Ar-purged solutions, oxygen originating from reaction (5) will be able to participate in the photodegradation. If all the added H_2O_2 undergoes reduction, the following stoichiometry will follow



In this case, two electrons will be scavenged per molecule of H_2O_2 . The lower limit for the H_2O_2 to quinoline ratio in this case is 24.

3.4. Effect of pH on the rate of TOC reduction

After the addition of FeCl_3 (1.5 mM) to quinoline (1 mM), a value of $\text{pH} \sim 3$ is obtained. At more acidic pH values, the photodegradation of quinoline slows down as shown in Fig. 8. In separate experiments, it was found that the pH used had no effect on the rate of H_2O_2 consumption. This suggests that, at more acidic pH, the reactions leading to O_2 formation become favourable.

3.5. Effect of the light intensity on the photodegradation. TOC decrease observed with a Suntest simulator

Fig. 9 shows the TOC reduction for the solution used in Fig. 8 (pH 3). The values plotted were taken at different times after the initial addition of H_2O_2 . The Suntest solar simulator was used as light source in Fig. 9. The points in the curve correspond to the full utilization of the H_2O_2 initially added. In agreement with Fig. 5, the TOC values are different for light and dark experiments. The results indicate a quantitative dependence between the light intensity and TOC reduction. As observed in Fig. 6 and reactions (3)–(6), the effect of the light intensity is important in the photoreaction of Fe^{3+} and H_2O_2 , controlling the efficiency and availability of the oxidant in the solution during the photoassisted Fenton reaction [12–14].

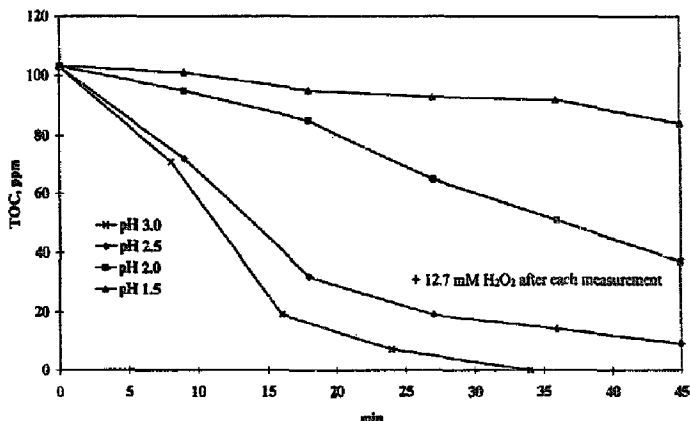


Fig. 8. Effect of pH on the degradation of quinoline for the same solution as used in Fig. 5.

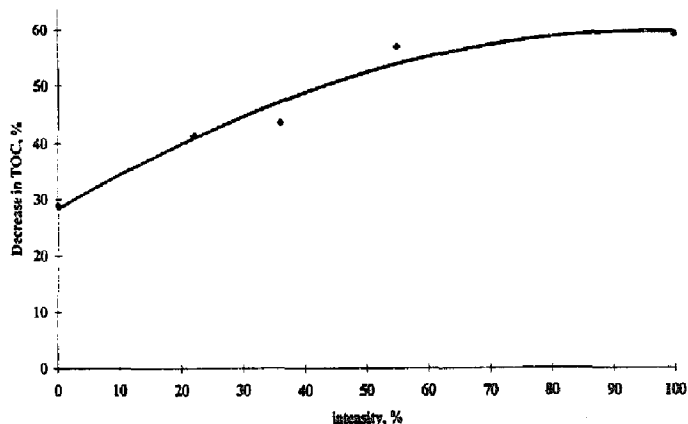


Fig. 9. Decrease in TOC of the quinoline solution used in Fig. 8 on exposure to solar-simulated irradiation as a function of the applied light intensity.

3.6. Nature of the products observed during mineralization in homogeneous medium

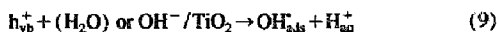
Fig. 10 presents the accelerated light-induced CO_2 evolution for the quinoline solution used in Fig. 5. The stoichiometric amount of carbon mineralizes within approximately 30 min. This agrees with the decrease in the TOC values observed in the solution. The data presented in Fig. 10 correspond to a stoichiometric ratio of quinoline to CO_2 of 1 : 9.

Fig. 11 presents the data for nitrate evolution during the photoassisted degradation of the solution used in Fig. 10. Nitrate forms rapidly and is the only N-containing product observed in the oxidative reaction medium. Subsequently, 80% of this intermediate decomposes within 15 min. Nitrite and ammonia are not observed, but N_2 is evolved. Interestingly, nitrate degradation occurs within the range of the secondary slow C–N hydrolysis reaction(s) reported previously in Fig. 5.

3.7. Heterogeneous degradation of quinoline via irradiated TiO_2 suspensions

The degradation of quinoline solutions is also possible using TiO_2 suspensions as shown in Fig. 12. The addition of H_2O_2 alone in the dark or light does not lead to efficient quinoline degradation. However, when this oxidant is added to a TiO_2 suspension, effective degradation is observed. Photodegradation times of about 2 h are observed in Fig. 12. This is four times longer than that obtained using the Fenton reagent with the same irradiation source (see Fig. 5).

The use of TiO_2 semiconductor particles has been extensively reported during the last decade for the heterogeneous degradation of pollutants [2,3,21]. Titania absorbs light below 385 nm leading to the production of OH^\cdot radicals on the surface (holes in the valence band oxidize surface OH^- groups as shown below)



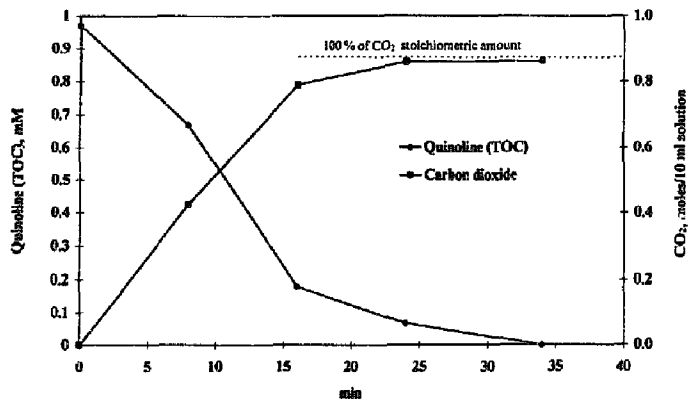


Fig. 10. Evolution of CO₂ on exposure to light when the solution used in Fig. 5 is irradiated with an Hg lamp. The TOC decrease is shown on the left axis.

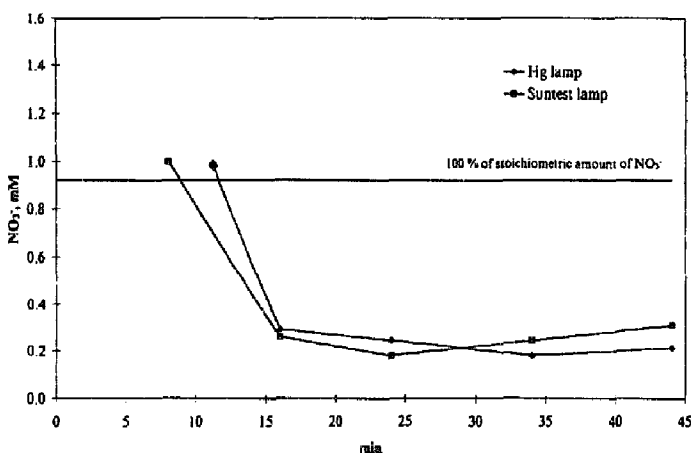


Fig. 11. Nitrate evolution as a function of time during the photodegradation of a quinoline (0.95 mM) solution in the presence of H₂O₂ (12.7 mM) and FeCl₃ (1.5 mM).

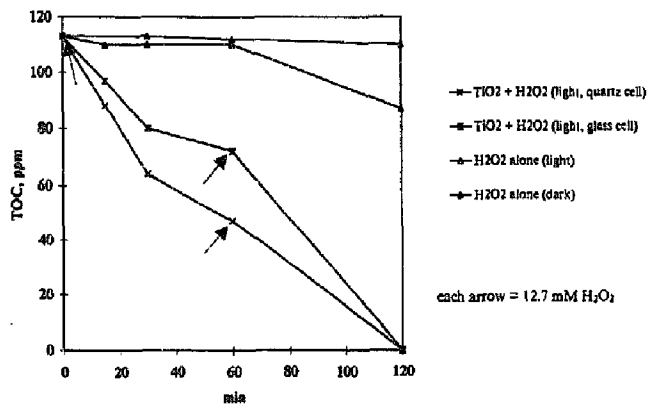


Fig. 12. Heterogeneous photodegradation as a function of time for a quinoline (1.16 mM) suspension using TiO₂ Degussa P-25 (1 g l⁻¹) in the presence of H₂O₂ (12.7 mM) at pH 3.

Fig. 12 suggests that these radicals plus the radicals due to H_2O_2 addition participate in the degradation. Other processes may also take place through reaction intermediates on illuminated TiO_2 slurries. However, we were interested only in optimizing and comparing the time span of the heterogeneous and homogeneous processes.

4. Conclusions

The photo-oxidation of quinoline via Fenton-like reagents has been reported in this study. The complete mineralization proceeds with the formation of CO_2 , water, nitrate and N_2 . The Fe^{3+} ion-based photo-Fenton reagent suitably accelerates the degradation kinetics and the system is catalytic rather than stoichiometric in iron. The pertinent reactions leading to degradation within minutes have been described. This observation and the fact that light reactions are effective in activating quinoline degradation provide the basis for possible practical applications. The use of H_2O_2 as oxidant is discussed. The photocatalytic degradation of quinoline proceeds at a faster rate than that observed with adapted microbial strains reported extensively [1–3].

Acknowledgements

This work was supported by Grant No. EV5V-CT93-0249 from the Commission of the European Communities (OFES No. 950031, Bern) and the INTAS Cooperation Project Grant No. 094-642 (Brussels).

References

- [1] N. Serpone, *Res. Chem. Intermed.* 9 (1954) 953.
- [2] G. Helz, G. Zepp, D. Crosby, *Aquatic and Surface Photochemistry*, Lewis, Boca Raton, FL, 1995.
- [3] C. Pulgarin, J. Kiwi, *Chimia* 50 (1996) 50.
- [4] J. Kiwi, C. Pulgarin, P. Peringer, *J. Appl. Catal. Environ.* 3 (1993) 85.
- [5] J. Bandara, J. Kiwi, C. Pulgarin, G.-M. Pajonk, P. Aibers, *Environ. Sci. Technol.* 30 (1996) 1261.
- [6] R. Andreozzi, M. D'Amore, *Water Res.* 26 (1992) 639.
- [7] C. Miller, R. Valentine, *Water Res.* 29 (1995) 353.
- [8] M. Fowler, J. Barker, L. Snowden, *Org. Geochem.* 22 (1994) 641.
- [9] D. Liu, E. Nagy, *Environ. Toxic. Water Qual.* 7 (1992) 355.
- [10] E. Godsy, D. Galic, *Ground Water* 30 (1992) 232.
- [11] J. Kiwi, C. Morrison, *J. Phys. Chem.* 88 (1984) 6146.
- [12] Ch. Walling, R. Johnson, *Acc. Chem. Res.* 8 (1975) 125.
- [13] C. Pulgarin, J. Kiwi, *Langmuir* 11 (1995) 519.
- [14] V. Nadochenko, J. Kiwi, *J. Photochem. Photobiol. A: Chem.* 99 (1996) 145.
- [15] R. Weast (Ed.), *CRC Handbook of Chemistry and Physics*, 59th edn., CRC Press, Boca Raton, FL, 1978.
- [16] A. Nedoloujko, J. Kiwi, *J. Photochem. Photobiol. A: Chem.* 211 (1997) 141.
- [17] Ch. Maillard, Ch. Guillard, P. Fichat, M.A. Fox, *New J. Chem.* 16 (1992) 821.
- [18] J. Bandara, C. Morrison, J. Kiwi, C. Pulgarin, P. Peringer, *J. Photochem. Photobiol. A: Chem.* 99 (1996) 57.
- [19] N. Rath, E. Holt, K. Tanimura, *J. Chem. Soc., Dalton Trans.* 11 (1986) 2303.
- [20] D. Sawyer, K. Chang, A. Llobet, Ch. Redman, D. Barton, *J. Am. Chem. Soc.* 115 (1993) 5817.
- [21] C. Morrison, J. Bandara, J. Kiwi, *J. Adv. Oxid. Technol.* 12 (1996) 160.